

## RESEARCH ARTICLE

# Design of patch antenna with polarization control module to achieve broad 3-dB gain bandwidth over entire AR range

Doyoung Jang<sup>1</sup> | Sungjun Yoo<sup>2</sup> |  
Hosung Choo<sup>1</sup> 

<sup>1</sup>School of Electronic and Electrical Engineering, Hongik University, Seoul, South Korea

<sup>2</sup>Advanced Defense Technology Research Institute Quantum Physics Technology Directorate, Agency for Defense Development, Daejeon, South Korea

## Correspondence

Hosung Choo, School of Electronic and Electrical Engineering, Hongik University, Seoul, South Korea  
Email: hschoo@hongik.ac.kr

## Funding information

Agency for Defense Development; Defense Acquisition Program Administration

## Abstract

This article proposes a novel patch antenna using a polarization control module to achieve a broad matching bandwidth and broad 3-dB gain bandwidth over the entire axial ratio (AR) range. The proposed antenna consists of a shorted radiating patch, an L-shaped indirect feed, and a polarization control module that can adjust AR properties over the entire AR range ( $-1 < AR < 1$ ) with a broad 3-dB gain bandwidth for use in various practical applications. The measured results demonstrate that the proposed antenna can adjust the polarization properties with a broadband matching bandwidth of more than 27% (370 MHz) and a broad 3-dB gain bandwidth greater than 26% (351 MHz) over the entire AR range.

## KEYWORDS

antennas, broadband antennas, patch antennas, polarization control

## 1 | INTRODUCTION

Microstrip patch antennas have been widely adopted for various applications, such as the Global Navigation Satellite System (GNSS), Satellite Digital Audio Radio Service (SDARS), and mobile communications, due to their low profile, low cost, and ease of fabrication.<sup>1-4</sup> However, conventional patch antennas are limited in their ability to cover a wide range of applications because of their narrow bandwidth characteristics. To improve bandwidth properties of the patch antennas, various broadband techniques, such as using slotted patches, air gap, and L-shaped indirect probe feed structures, have been introduced.<sup>2,5-10</sup> In addition to the broad matching characteristics, patch antennas should have suitable polarization within the required frequency range according to each application. Various polarizations adjustment techniques, such as using parasitic elements, two-port with a branch-line coupler,<sup>11</sup> and pin-diode<sup>12</sup> have been proposed to obtain axial ratio (AR) characteristics including linear, right-hand circular (RHC), left-hand circular (LHC), and elliptical polarizations (EP). However, the matching bandwidth and the 3-dB gain bandwidth for each polarization are often too narrow for practical applications.<sup>13</sup>

In this article, we propose a novel patch-antenna design with broad matching bandwidth and broad 3-dB gain bandwidth, which can adjust AR properties for various practical applications. The proposed antenna consists of a shorted radiating patch, an L-shaped indirect feed, and a polarization control module. To simultaneously achieve both the broad matching bandwidth and the broad 3-dB gain bandwidth, the shorted radiating patch is designed to be electromagnetically coupled with the L-shaped probe, resulting in semi-uniform coupling field strength over the broad bandwidth between the feed and the patch. In addition, the polarization control module is located on the outer perimeter of the shorted radiating patch to induce a magnetic current between the radiating patch and the polarization control module. This allows to adjust the polarization characteristics by controlling the magnetic current distributions in accordance with the angle of polarization control module. To verify the feasibility of the proposed antenna structure, four polarization control modules for four different polarizations were fabricated, and their gains, radiation patterns, and ARs were measured in a full anechoic chamber. Herein, the 3-dB gain bandwidth is obtained using the generalized gain depending on AR. The proposed antenna achieves a broad 3-dB gain bandwidth of

greater than 26% and a broad matching bandwidth of more than 27%. We also confirmed that desired polarization can be obtained at frequencies other than a particular frequency by replacing the polarization control module. The results demonstrate that the proposed antenna can adjust the polarization properties with the broadband matching characteristics and the broad 3-dB gain bandwidth covering the entire AR range.

## 2 | PROPOSED ANTENNA DESIGN

Figure 1 presents the geometry of the proposed antenna with a broad matching bandwidth and a broad 3-dB gain bandwidth, which consists of a shorted radiating patch, an L-shaped indirect feed, and a polarization control module. The

shorted radiating patch with width  $w$  and length  $l$  is located at height  $h$  above the ground. The shorted radiating patch is designed to be electromagnetically coupled with the L-shaped probe to achieve semi-uniform coupling field intensity over the broad bandwidth between the feed and the patch. As is well known, the length of the shorted radiating patch is reduced by half-compared to the conventional patch antenna. The polarization control module is then located outside the perimeter of the radiating patch, which is separated by distance  $d$ . The module is detachable and fixed with four supporting posts as shown in Figure 1. The polarization control module can be mounted on the patch in a configuration that maximizes the received power. The polarization control module with a rectangular loop shape has a width of  $w_p$  and a length of  $l_p$ . The polarization control module is divided into two parts by two gaps with length and width of  $g$  and  $t$ , respectively. The position of the gaps is determined by the angle  $\phi_g$ . This configuration allows the polarization characteristics to be adjusted by controlling the amplitude and phase of the magnetic current between the radiating patch and the polarization control module, while varying the angle  $\phi_g$ . Detailed design parameters are optimized by a genetic algorithm (GA)<sup>14,15</sup> in conjunction with the FEKO EM simulator,<sup>16</sup> and the optimized values are listed in Table 1.

Figure 2 illustrates the AR and bore-sight gain of the proposed antenna according to  $\phi_g$ . The “+” marker and solid line imply the measured and simulated AR, respectively. When the angle  $\phi_g$  changes from  $-25^\circ$  to  $0^\circ$ , the polarization maintains the left-hand polarization, and as  $\phi_g$  approaches  $0^\circ$ , the polarization becomes linear polarization (LP). When  $\phi_g$  is greater than  $0^\circ$ , the polarization characteristics change

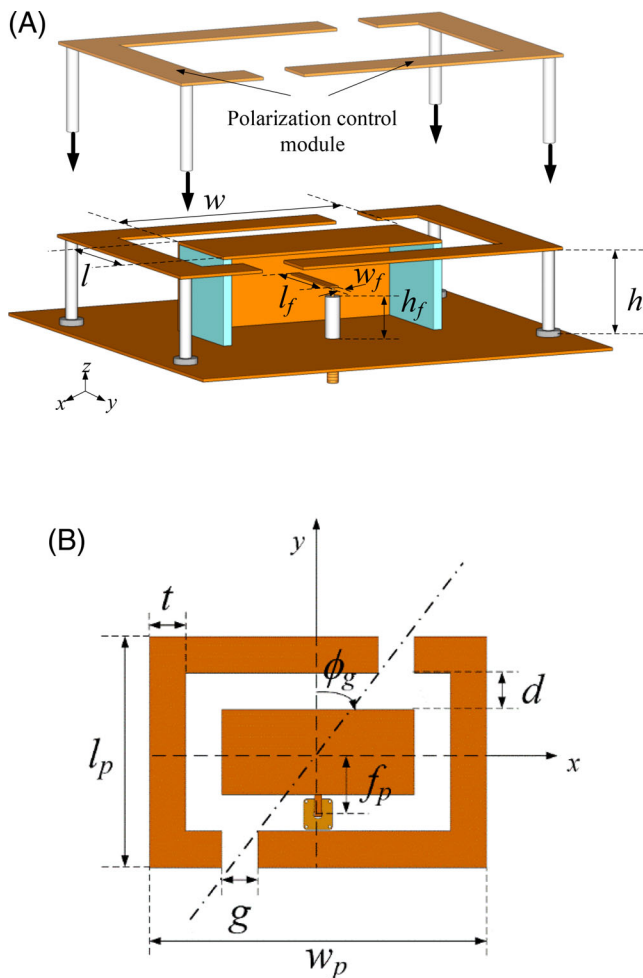


**FIGURE 1** Geometry of the proposed antenna with polarization control module. A, Isometric view. B, Top view [Color figure can be viewed at wileyonlinelibrary.com]

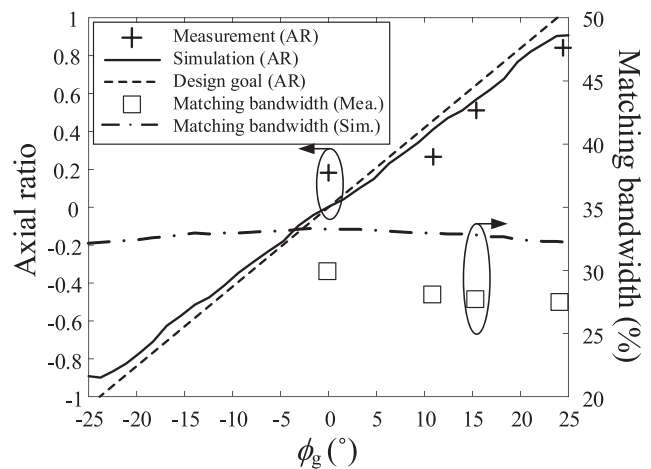


**FIGURE 2** Effects of parameter  $\phi_g$  on axial ratio (AR) and matching bandwidth

**TABLE 1** Optimized values of the proposed antenna

Parameter	$w$	$l$	$h$	$w_f$	$l_f$	$h_f$	$f_p$	$w_p$	$l_p$	$t$	$d$	$g$	$\phi_g$
Value (mm)	81	34	20.3	5	32.4	13.5	17	139.1	92.1	19.5	9.6	22.1	$-25^\circ \sim 25^\circ$

to right-hand polarization. The polarization control module at  $\phi_g = 24.5^\circ$  achieves the maximum AR of 1 (RHCP), and the minimum AR of  $-1$  (LHCP) is obtained at  $\phi_g = -24.5^\circ$ . The targeted AR ranging from  $-1$  to  $1$  can be obtained by varying  $\phi_g$  in the range of  $-24.5^\circ < \phi_g < 24.5^\circ$ . As shown in Figure 2, the measured and simulated ARs of the proposed antenna are good agreement with the ARs of the design goal (dashed line). The measured ('□' marker) and simulated (dash-dotted line) matching bandwidths also show the broadband characteristics. These results demonstrate that the variety of polarizations can be obtained while

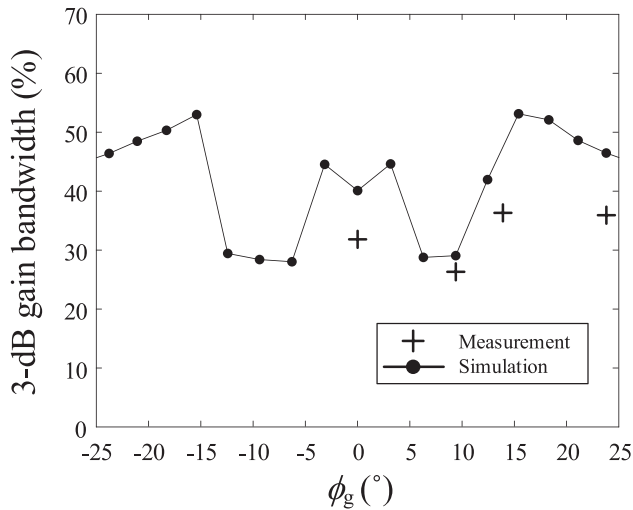


**FIGURE 3** Effects of parameter  $\phi_g$  on 3-dB gain bandwidth

maintaining the measured matching bandwidth of over 27% (370 MHz). To verify the broadband gain property of the proposed antenna, the 3-dB gain bandwidth is calculated according to AR characteristics, and the gain for each AR is determined by:

$$G(AR) = 20 \cdot \log_{10} \left[ \eta_e \cdot \frac{2\pi}{P_{rad}} \cdot \sqrt{\frac{\epsilon_0}{\mu_0}} \cdot \frac{|E_\theta^\circ(\theta, \phi) + E_\phi^\circ(\theta, \phi) \cdot e^{j\frac{\pi}{2} \cdot AR}|}{\sqrt{2}} \right] \quad (-1 \leq AR \leq 1) \quad (1)$$

where  $E_\theta^\circ$  and  $E_\phi^\circ$  are  $\theta$  and  $\phi$  components of the electric fields that are normalized with respect to the distance.  $P_{rad}$  and  $\eta_e$  are the radiated power in all directions and the antenna radiation efficiency, respectively.  $G(AR)$  is the gain for a particular AR value, which is calculated by considering for a specific AR. As the gains of CP antennas are evaluated as an RHC gain ( $AR = 1$ ) or an LHC gain ( $AR = -1$ ), an antenna with a specific AR ( $-1 < AR < 1$ ) should be evaluated as a generalized gain  $G(AR)$  in consideration of its AR. Since  $G(AR)$  is a generalized form of the equation for RHC or LHC gains,  $G(AR)$  reflects gains with the entire variation of AR from  $-1$  to  $1$ . For example, if AR is  $\pm 1$ , the equation becomes the RHC gain or LHC gain, while AR is  $0$ , it becomes the gain for LP. By investigating the generalized gain  $G(AR)$  for desired specific AR ratios, 3-dB gain bandwidths more than 26% over the entire AR range are observed, as shown in Figure 3, even if the module configuration changes.

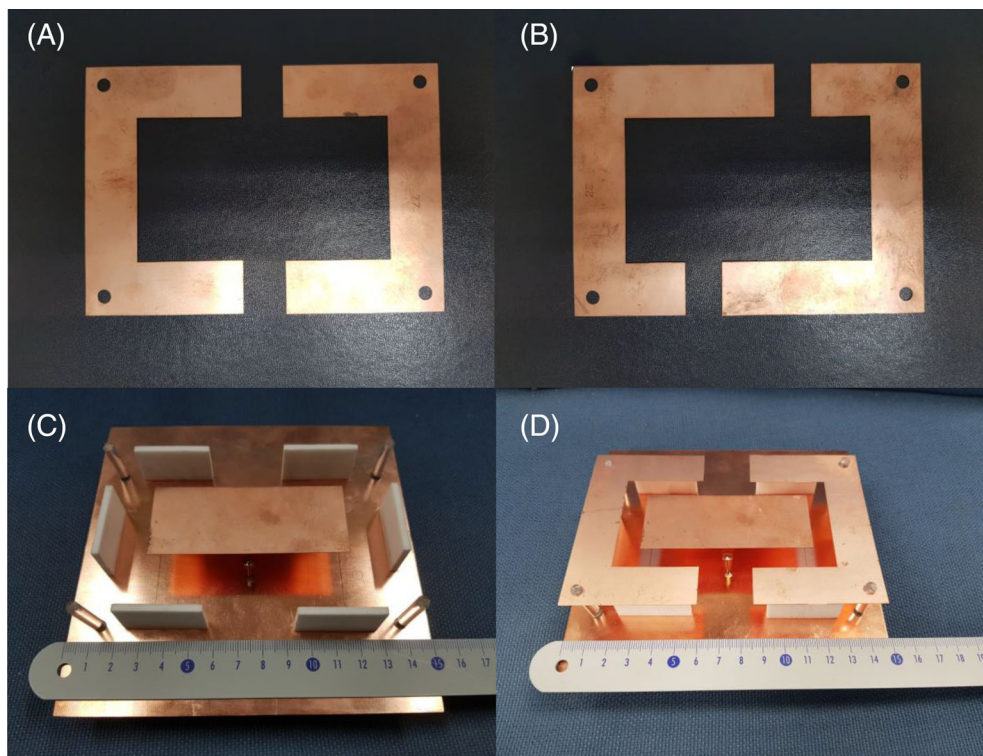


**FIGURE 4** Photographs of the fabricated antennas. A, Polarization control module for LP. B, Polarization control module for CP. C, Patch antenna with support posts and Styrofoam. D, Fabricated antenna [Color figure can be viewed at [wileyonlinelibrary.com](http://wileyonlinelibrary.com)]

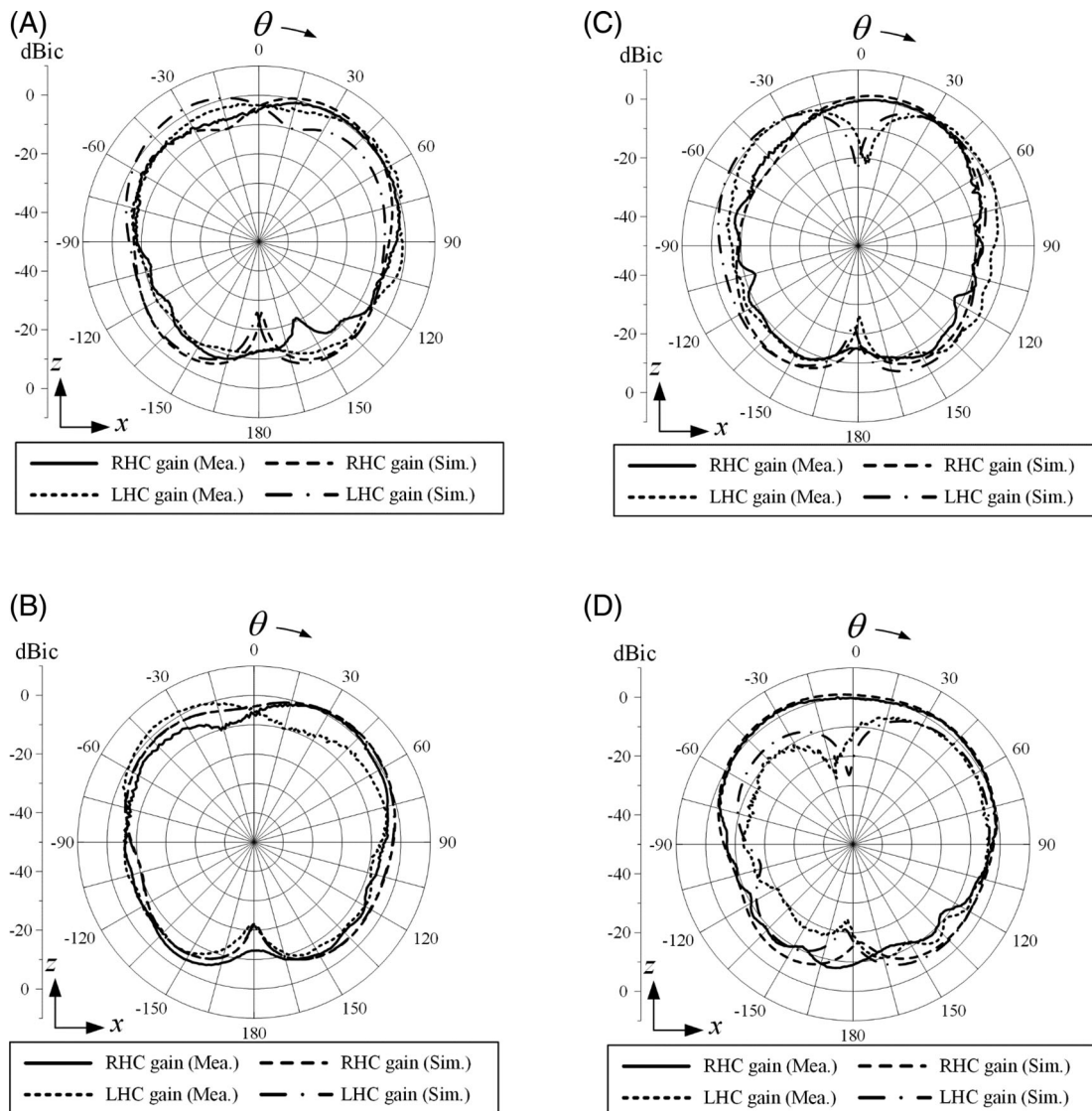
### 3 | PROPOSED ANTENNA FABRICATION AND MEASUREMENT

Figure 4 shows photographs of the fabricated antenna with polarization control modules. The configurations of the modules shown in Figure 4A,B can make LP and CP, respectively. The proposed antenna includes four plastic support posts and Styrofoam walls to facilitate replacement of the polarization control model, as shown in Figure 4C. When the module is mounted on the antenna, the proposed antenna is configured as shown in Figure 4D, which can achieve the broad matching bandwidth and the broad 3-dB gain bandwidth.

Figure 5 presents the measured 2-D radiation patterns of the proposed antenna in a full anechoic chamber, when the two different polarization modules for LP and CP are utilized. With the polarization control module for LP, the measured bore-sight RHC and LHC gains at  $zx$ -plane

and  $zy$ -plane are  $-2.7$  dBic and  $-3.5$  dBic at 1.575 GHz, respectively, as shown in Figure 5A,B. The difference between the RHC gain and LHC gain is small, which means that the proposed antenna has LP. With the polarization control module for CP as in Figure 5C,D, the measured RHC and LHC gains at  $zx$ -plane and  $zy$ -plane are 0.1 dBic and  $-13.6$  dBic, respectively at the same frequency. The results indicate that the antenna of this configuration has CP, and the measurements agree well with the simulation data.

The proposed polarization control module can control polarization not only at 1.575 GHz but also at different frequencies. To verify that the proposed antenna can obtain the CP polarization at other frequencies, we designed three different polarization control modules. Figure 6 shows the AR according to change the polarization control module for three different frequencies. The solid line, dashed, and dotted line indicate simulated AR values when the proposed antenna combines modules to have CPs at 1.2, 1.4, and



**FIGURE 5** Radiation pattern of the fabricated antennas. A, LP configuration ( $zx$ -plane). B, LP configuration ( $zy$ -plane). C, CP configuration ( $zx$ -plane). D, CP configuration ( $zy$ -plane)

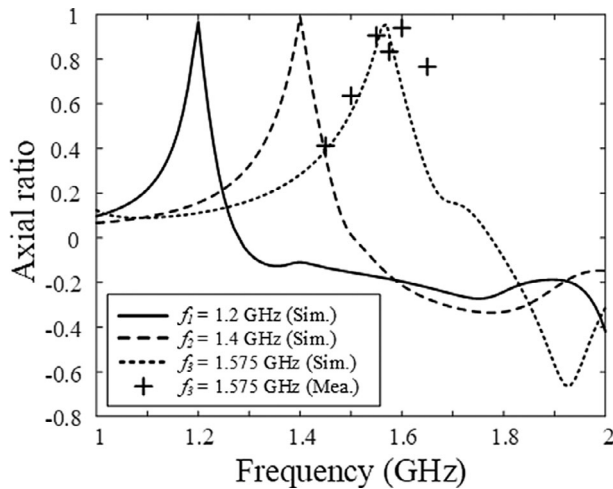


**FIGURE 6** Axial ratio according to change the polarization control module

1.575 GHz, respectively. The measured result (“+” marker) is added for comparison with the simulation at 1.575 GHz. As a result, the peak value of AR appears at operating frequencies. The result demonstrates that the polarization characteristics can also be adjusted at target frequency by replacing the polarization control module.

## 4 | CONCLUSION

A novel patch-antenna design has been investigated to achieve a broad matching bandwidth and a broad 3-dB gain bandwidth over the entire AR range. The proposed antenna consists of a shorted radiating patch, an L-shaped indirect feed, and a polarization control module. The results demonstrated that the proposed antenna can maintain a 3-dB gain bandwidth above 26% and matching bandwidth over 27% over the entire AR range by controlling the magnetic current distributions in accordance with the angle of the polarization control module.

## ACKNOWLEDGMENTS

This work was supported in part by the Research Fund of Signal Intelligence Research Center supervised by the Defense Acquisition Program Administration, Agency for Defense Development of Korea.

## ORCID

Hosung Choo  <https://orcid.org/0000-0002-8409-6964>

## REFERENCES

[1] Yeom I, Jung YB, Jung CW. Wide and dual-band MIMO antenna with omnidirectional and directional radiation patterns for indoor access points. *J Electromagn Eng Sci.* 2019;19:20-30.

[2] Kim J, Sung Y. Dual-band microstrip patch antenna with switchable orthogonal linear polarizations. *J Electromagn Eng Sci.* 2018;18(4):215-220.

[3] Bilgic MM, Yegin K. Modified annular ring antenna for GPS and SDARS automotive applications. *IEEE Antennas Wireless Propag Lett.* 2015;15:1442-1445.

[4] Huang H, Li X, Liu Y. A low-profile, dual-polarized patch antenna for 5G MIMO application. *IEEE Trans Antenna Propag.* 2019;67(2):1275-1279.

[5] Rajanna PKT, Rudramuni K, Kandasamy K. A wideband circularly polarized slot antenna backed by a frequency selective surface. *J Electromagn Eng Sci.* 2019;19:166-171.

[6] Yang F, Zhang X-X, Ye X, Rahmat-samii Y. Wide-band E-shaped patch antennas for wireless communications. *IEEE Trans Antenna Propag.* 2001;49:1094-1100.

[7] Jang D, Yoo S, Wang J, Choo H. Design of a 16-element array antenna with a planar L-shaped probe for a direction of arrival estimation of the unidentified broadband signal. *Microwave Opt Tech Lett.* 2019;61(10):2315-2322.

[8] Mak KM, Lai HW, Luk KM. A 5G wideband patch antenna with antisymmetric L-shaped probe feeds. *IEEE Trans Antennas Propag.* 2018;66(2):957-961.

[9] Kishk AA, Lee KF, Mok WC, Luk K-M. Wide-band small size microstrip antenna proximately coupled to a hook shape probe. *IEEE Trans Antennas Propag.* 2004;52(1):59-65.

[10] Wu Z-H, Lou Y, Yung EK-N. A circular patch fed by a switch line balun with printed L-probes for broadband CP performance. *IEEE Antennas Wireless Propag Lett.* 2007;6:608-611.

[11] Liu J, Li J-Y, Xu R, Zhou S-G. A reconfigurable printed antenna with frequency and polarization diversity based on Bow-Tie dipole structure. *IEEE Antennas Propag.* 2019;67(12):7628-7632.

[12] Akkermans JAG, Herben MHAI. Millimeter-Wave antenna with adjustable polarization. *IEEE Antennas Wireless Propag Lett.* 2008;7:539-542.

[13] Yoo S, Choo H, Byun G. Design of mechanically rotatable microstrip patch antennas using an asymmetric polariser for adaptive polarisation adjustment. *IET Microwaves Antennas Propag.* 2019;13(8):1122-1128.

[14] Pazokian M, Komjani N, Karimipour M. Broadband RCS reduction of microstrip antenna using coding frequency selective surface. *IEEE Antennas Wireless Propag Lett.* 2018;17(8):1382-1385.

[15] Kim J-Y, Chun D-W, Ryu CJ, Lee H-Y. Optimization methodology of multiple air hole effects in substrate integrated waveguide applications. *J Electromagn Eng Sci.* 2018;18(3):160-168.

[16] FEKO EM Simulation Software, Altair Engineering Inc., 2019. [Online]. Available: <http://www.altair.co.kr>.

**How to cite this article:** Jang D, Yoo S, Choo H. Design of patch antenna with polarization control module to achieve broad 3-dB gain bandwidth over entire AR range. *Microw Opt Technol Lett.* 2020;62: 2606–2610. <https://doi.org/10.1002/mop.32360>